THE ASTRONOMICAL JOURNAL, 121:327–336, 2001 January

METAL ABUNDANCES OF RED CLUMP STARS IN OPEN CLUSTERS. I. NGC 6819[1]

ANGELA BRAGAGLIA,[2] EUGENIO CARRETTA,[3] RAFFAELE G. GRATTON,[3] MONICA TOSI,[2] GIOVANNI BONANNO,[4] PIETRO BRUNO,[4] ANTONIO CALÌ,[4] RICCARDO CLAUDI,[3] ROSARIO COSENTINO,[4] SILVANO DESIDERA,[5] GIANCARLO FARISATO,[3] MAURO REBESCHINI,[3] AND SALVO SCUDERI[4]

Received 2000 August 29; accepted 2000 September 19

ABSTRACT

We present an analysis of high-dispersion spectra ($R \sim 40{,}000$) of three red clump stars in the old open cluster NGC 6819. The spectra were obtained with SARG, the high-dispersion spectrograph of the Telescopio Nazionale Galileo. The spectra were analyzed using both equivalent widths measured with an automatic procedure and comparisons with synthetic spectra. NGC 6819 is found to be slightly metal-rich ([Fe/H] $= +0.09 \pm 0.03$, internal error); there are no previous high-resolution studies to compare. Most element-to-element abundance ratios are close to solar; we find a slight excess of Si and a significant Na overabundance. Our spectra can also be used to derive the interstellar reddening toward the cluster by comparing the observed colors with those expected from line excitation: we derive $E(B-V) = 0.14 \pm 0.04$, in agreement with the most recent estimate for this cluster.

Key words: open clusters and associations: individual (NGC 6819) — stars: abundances — stars: fundamental parameters — techniques: spectroscopic

1. INTRODUCTION

Open clusters (OCs) are excellent tools to infer the evolution of our Galaxy from both the chemical and structural points of view because they provide information on the distribution of the chemical abundances in the disk, on the average ages at various galactic locations, on the initial mass function, and on the interactions between thin and thick disks (see, e.g., Mayor 1976; Panagia & Tosi 1981; Friel 1995; Luhman et al. 2000). The major advantage of using OCs rather than field stars to derive these quantities resides in the circumstance that (1) their current galactic location is not too different from where they were born and (2) the distances, ages, and metallicities of field stars located beyond a limited radius from the Sun are highly uncertain.

OCs probably represent the best means to understand how element abundances change with time and with location in the Galaxy. Several years ago, it was suggested that young OCs show steeper negative abundance gradients with galactocentric distance than old clusters (Mayor 1976; Panagia & Tosi 1981). However, later extensive studies (e.g., Friel & Janes 1993) have suggested that the gradient slope is roughly independent of the cluster age. A striking characteristic of Friel & Janes's sample is that at each Galactic radius the oldest clusters happen to be also the most metal-rich ones. This result, if confirmed, would have remarkable implications on our understanding of the Galaxy evolution, since it is opposite of any intuitive age−metallicity relation derivable from steady state scenarios and suggests the existence of short, intense phenomena that may alter local evolutions significantly. A caveat of these results is that they can be strongly affected by several uncertainties also related to the lack of homogeneity in the derivation of the cluster parameters (age, metallicity, distance, and reddening). As discussed, e.g., by Bragaglia et al. (2001), use of literature values can lead to a confusing picture; for instance, ages derived with different techniques or isochrones may be not only uncertain in absolute value but also in ranking.

To overcome this problem, we are homogeneously analyzing with great accuracy a sample of open clusters that lie at various galactic locations and cover a wide range in age and metallicity. We derive the age, distance, reddening, and approximate metallicity of these systems from deep photometry combined with the synthetic color-magnitude diagram method (see, e.g., Sandrelli et al. 1999 and references therein), while accurate element abundance determination is based on high-resolution spectroscopy. The final sample of OCs necessary to allow for significant statistics on the abundance gradient at various epochs should include at least 30 objects.

In this paper we present the abundances derived from high-resolution spectroscopy of the first cluster of the sample: NGC 6819, an intermediate–age cluster (age $\simeq$ 2.3–3.1 Gyr) with R.A. $= 19^{h}41^{m}$, decl. $= +40°12'$ (J2000.0), $(l, b) = (73.°98, 8.°47)$, and Galactocentric distance 8.2 kpc. A recent reference for photometry and derivation of distance and age is Rosvick & VandenBerg (1998). The observations have been performed with SARG, the new high-dispersion spectrograph at the Italian Telescopio Nazionale Galileo (TNG), and this is the first paper in which data acquired with this instrument are presented.

2. OBSERVATIONS AND DATA REDUCTION

Spectra were obtained of two clump stars in 2000 July and of one in 2000 August, during the second and third commissioning runs of SARG, the new high-dispersion spectrograph at the 3.5 m TNG in La Palma (Spain). The stars were selected (using BDA, the database for Galactic open clusters; Mermilliod 1995) among fiducial cluster

[1] Based on observations made with the Italian Telescopio Nazionale Galileo (TNG) operated on the island of La Palma by the Centro Galileo Galilei of the Consorzio Nazionale per l'Astronomia e l'Astrofisica at the Spanish Observatorio del Roque de los Muchachos of the Instituto de Astrofisica de Canarias.

[2] Osservatorio Astronomico di Bologna, via Ranzani 1, I-40127 Bologna, Italy; angela@bo.astro.it, tosi@bo.astro.it.

[3] Osservatorio Astronomico di Padova, Vicolo Osservatorio 5, I-35122 Padova, Italy; carretta@pd.astro.it, gratton@pd.astro.it, claudi@pd.astro.it, farisato@pd.astro.it, rebeschini @pd.astro.it.

[4] Osservatorio Astrofisico di Catania, Università di Catania, via S. Sofia 78, I-95125, Catania, Italy; gbo@sunct.ct.astro.it.

[5] Dipartimento di Astronomia, Università di Padova, Vicolo Osservatorio 5, I-35122 Padova, Italy; desidera@pd.astro.it.

TABLE 1

INFORMATION ON THE OBSERVED STARS

Ident	R.A. (2000.0)	Decl. (2000.0)	V	$B-V$	Prob. Memb.	Date	UT (Init.)	Exposure (s)	RV (kms^{-1})
333.....	19 41 20	+40 12 41	13.069	1.176	92	2000 Aug 17	00 45 41	3600	5.31
978.....	19 41 15	+40 11 05	12.869	1.149	90	2000 Jul 18	01 14 35	3600	5.96
979.....	19 41 17	+40 11 11	12.956	1.075	91	2000 Jul 18	02 20 19	3600	1.44

NOTES.—Units of right ascension are hours, minutes, and seconds, and units of declination are degrees, arcminutes, and arcseconds. RV values are heliocentric and derived from about 100 Fe I lines in each spectrum. Identification is taken from the BDA (Mermilliod 1995, an extension of the Auner 1974 numeration); photometry, from Rosvick & VandenBerg (1998); and membership, from Sanders (1972).

members selected from proper motions (Sanders 1972) and now confirmed by the velocities measured from our spectra. The most important data for the program stars are listed in Table 1 along with a summary of the spectral characteristics and the heliocentric radial velocities; Figure 1 gives the location of the stars in the color-magnitude diagram (*top*) and on the sky (*bottom*).

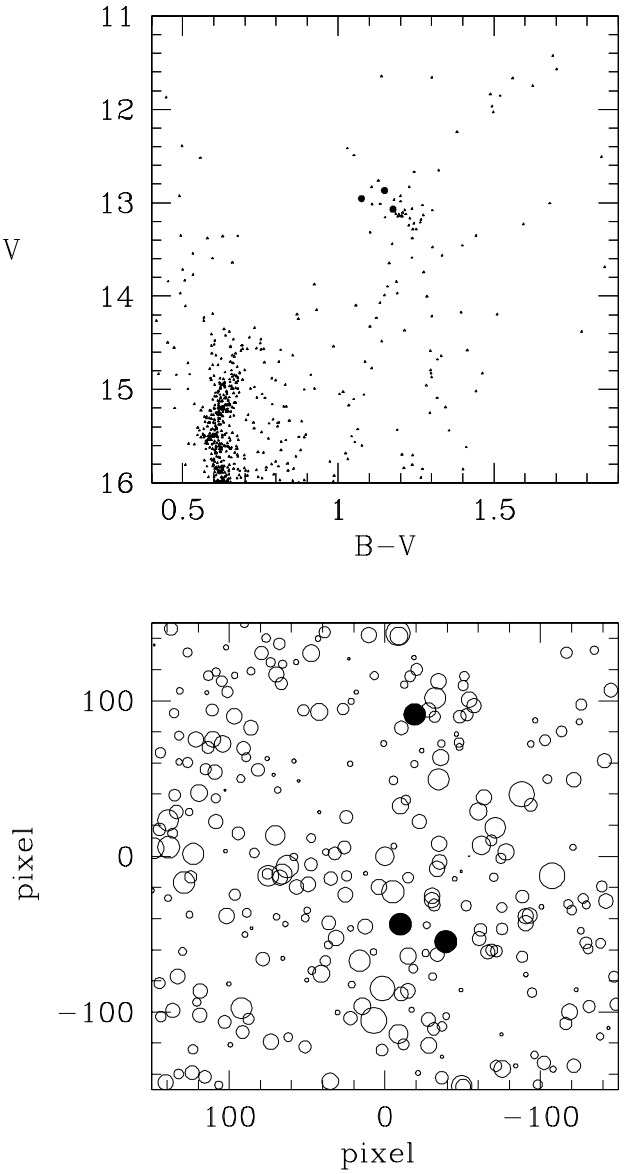

FIG. 1.—*Top*: CMD for NGC 6819, taken from Rosvick & VandenBerg (1998). The three observed stars are shown with a heavier mark. *Bottom*: cluster map (field of 2.8 arcmin^2, east on the left, north up) with the three observed clump stars plotted as filled circles; *from top to bottom*: 333, 979, and 978.

This being the first paper based on SARG data, a few details about the spectrograph and the observations are to be provided. SARG (Gratton et al. 2001) is a single-arm, white-pupil, cross-dispersed echelle spectrograph, permanently mounted on one of the arms of the TNG fork. It is fed by a suitable optical train from the Nasmyth focus. The spectrograph uses an R4 echelle grating in an off-plane, quasi-Littrow configuration that yields an *RS* product of 46,000 when coupled with the 100 mm spectrograph beam. Spectral resolution of SARG depends on the selected slit (a set of seven is available on the slit wheel, from 0.″27 to 1.″60), the maximum value being about 150,000. The present observations were obtained using a slit width of 300 μm, corresponding to 1.″60 projected on the sky. However, stellar images did not completely fill this wide slit. During the observations, the seeing value was about 0.″7. Since the guiding accuracy was not yet optimal (only manual guiding was available when the program spectra were acquired), the actual images over the 1 hr exposure time had an FWHM of about 1.″2, yielding a spectral resolution of about 40,000. This value is confirmed by measures of the FWHM of narrow telluric lines.

SARG is equipped with four grism cross-dispersers mounted on a wheel; the present observations were made using the yellow grism, which provides an almost complete spectral coverage from 4650 to 7900 Å, with only a small gap of about 40 Å near 6200 Å, due to the nonsensitive region between the two $4k \times 2k$ thinned, back-illuminated EEV CCDs located on the focal plane of the spectrograph. Minimum interorder separation is about 7″. To reduce readout noise and readout time, the CCDs were binned 4×4. With this choice, 2 pixel resolution is 36,000, a bit less than the FWHM of the spectral lines, so that the spectra are slightly undersampled. The spectra have a rather high background level, due to parasite light in the spectrograph not yet eliminated when they were acquired, which is well removed by the spectrum extraction procedure. The high background level has small impact on the spectra of these rather bright stars, and the final S/N $\sim$ 130 is that expected from photon noise.

Spectral extraction was done using standard IRAF routines[6] for echelle spectra. First, the two CCD were separated and reduced independently. The two-dimensional images were bias-subtracted (but not flat-fielded; the flats were extracted and used to check the quality of correction

[6] IRAF is distributed by the National Optical Astronomy Observatories, which are operated by the Association of Universities for Research in Astronomy, Inc., under contract with National Science Foundation.

done for the blaze function, with the ISA package; Gratton 1988) then cleaned from cosmic-ray hits and hot pixels using COSMICRAYS. Images were corrected for scattered light; the orders were then found (21 in the red CCD and 34 in the blue one), traced, and extracted, and the local sky background was subtracted. Wavelength calibration was performed using thorium lamp exposures taken once each night (the spectrograph is very stable, and furthermore precise radial velocities were not our goal), yielding an rms of about 0.009 Å in our wavelengths.

3. ANALYSIS AND ERROR ESTIMATES

3.1. *Equivalent Widths*

In our analysis, we used both equivalent widths (EWs) and spectral synthesis. Equivalent widths were used to derive the best set of atmospheric parameters (effective temperature from line excitation, gravity from the equilibrium of ionization, and microturbulence from trends with expected line strength; see Table 2) and elemental abundances. Comparisons with synthetic spectra were then used to check the adopted abundances.

Equivalent widths (see Table 3) were measured on the unidimensional, extracted spectral orders using an automatic routine within the ISA package, prepared by one of us (R. G. G.). Only the spectral region 5500–7200 Å was eventually used in the abundance analysis: continuum tracing is quite uncertain at shorter wavelengths at the resolution of our spectra, and diffraction fringes (not completely removed by our reduction procedure) make results from longer wavelengths uncertain. The routine for measuring equivalent widths works as follows. First, removal of the blaze function response is performed using a spline interpolating function. Then, a local continuum level is determined for each line by an iterative clipping average over a fraction (the highest ones) of the 200 spectral points centered on the line to be measured; after various tests, this fraction was set at $\frac{1}{4}$ for the spectra of NGC 6819. Second, the equivalent width for each line from an extensive list (including several hundred lines that are quite clean in the solar spectrum) is tentatively measured using a Gaussian fitting routine. Measures are rejected according to several criteria (e.g., if the central wavelength does not agree with that expected from a preliminary measure of the geocentric radial velocity or if the lines are too broad or too narrow). Third, the measured lines are used to draw a relationship between equivalent width and FWHM. Fourth, this relation is used to measure equivalent widths again, using a second Gaussian fitting routine that has only one free parameter (the equivalent width), since the central wavelength is fixed by the measured geocentric radial velocity and the FWHM is fixed by the relationship between equivalent width and FWHM. Again measures are rejected if residuals are too large, asymmetric, etc.

TABLE 2

ADOPTED ATMOSPHERIC PARAMETERS AND IRON ABUNDANCES

Star	$T_{\rm eff}$ (K)	log g (dex)	v_t (km s^{-1})	[Fe/H]
333.....	4835	2.61	1.54	0.11
978.....	4855	2.60	1.26	0.11
979.....	4740	2.72	0.98	0.11

These procedures allow one to obtain very stable measures of the EWs, with small random errors even when lines are in quite crowded spectral regions. However, systematic errors, related to the adopted reference continua, may be present. Comparisons with synthetic spectra convinced us that systematic errors in the finally adopted EWs are quite small, insofar as a suitable fraction of the points is used to determine the reference continuum level and rejection criteria on the used lines are kept strict.

Since the stars have similar atmospheric parameters, we may estimate (internal) errors in our equivalent widths by comparing values measured in different stars. Such a comparison is shown in Figure 2. By taking as a reference star 978 (which is the brightest and has the best spectrum), the rms scatter about the linear relationship is 10.9 and 10.5 mÅ for stars 333 and 979, respectively. Assuming that both sets of EWs have equal errors, we can estimate typical errors of 7.5 mÅ in our measured EWs.

3.2. *Atmospheric Parameters*

Equivalent widths and Kurucz model atmospheres (1995; models with the overshooting option switched off) were

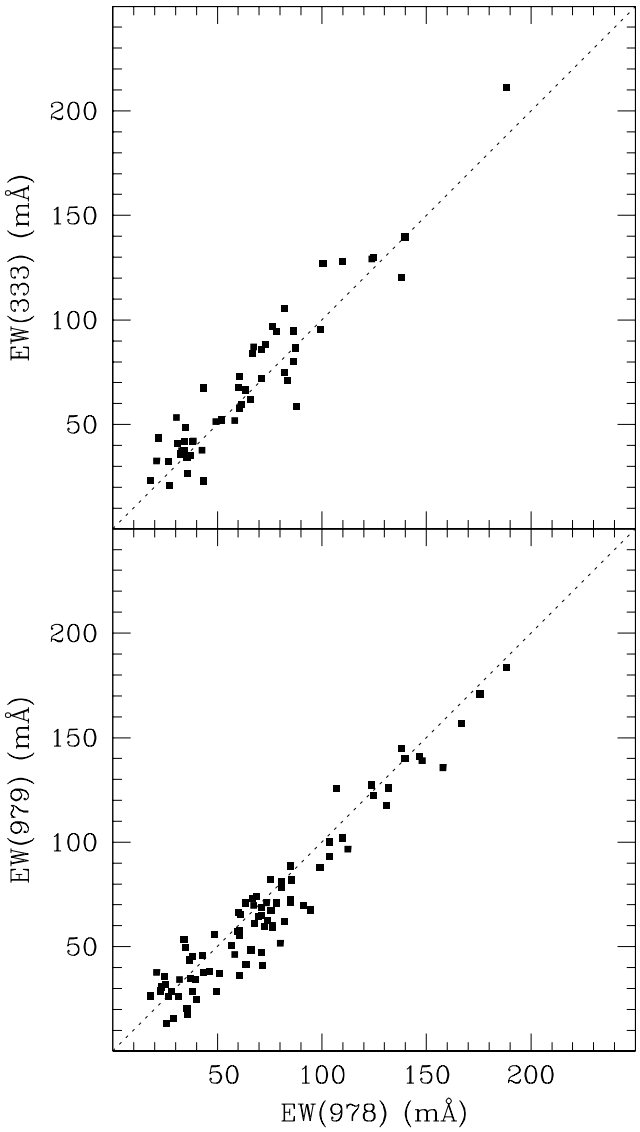

FIG. 2.—Comparisons between the equivalent widths measured for star 978 and those measured for star 333 (*top*) and 979 (*bottom*).

TABLE 3

EQUIVALENT WIDTHS

				333		978		979	
ELEMENT	λ	E. P.	log gf	EW (mÅ)	Abund.	EW (mÅ)	Abund.	EW (mÅ)	Abund.
Na I	5688.22	2.10	−0.37	0.0	0.00	0.0	0.00	151.5	6.32
Na I	6154.23	2.10	−1.57	109.4	6.77	0.0	0.00	105.1	6.81
Na I	6160.75	2.10	−1.26	120.2	6.60	138.4	6.96	144.6	7.04
Mg I.....	5528.42	4.34	−0.48	0.0	0.00	0.0	0.00	212.1	7.12
Mg I.....	5711.09	4.34	−1.71	138.0	7.50	0.0	0.00	0.0	0.00
Mg I.....	6318.71	5.11	−1.97	0.0	0.00	71.5	7.65	41.2	7.17
Mg I.....	6319.24	5.11	−2.20	0.0	0.00	0.0	0.00	37.0	7.32
Al I	6696.03	3.14	−1.32	0.0	0.00	80.2	6.44	51.6	5.95
Al I	6698.67	3.14	−1.62	58.1	6.35	0.0	0.00	60.6	6.40
Si I.....	5645.62	4.93	−2.14	62.0	7.72	65.9	7.83	0.0	0.00
Si I.....	5665.56	4.92	−2.04	0.0	0.00	0.0	0.00	73.2	7.98
Si I.....	5684.49	4.95	−1.65	92.8	7.76	0.0	0.00	88.8	7.90
Si I.....	5690.43	4.93	−1.87	58.4	7.39	87.6	7.95	0.0	0.00
SiII	5701.11	4.93	−2.05	67.8	7.72	60.0	7.63	66.4	7.87
Si I.....	5772.15	5.08	−1.75	0.0	0.00	85.1	7.93	88.5	8.13
Si I.....	5793.08	4.93	−2.06	66.7	7.71	63.8	7.71	71.2	7.96
Si I.....	5797.87	4.95	−2.05	0.0	0.00	0.0	0.00	53.7	7.65
Si I.....	5948.55	5.08	−1.23	0.0	0.00	107.1	7.78	125.5	8.16
Si I.....	6125.03	5.61	−1.57	51.3	7.70	49.4	7.69	0.0	0.00
Si I.....	6145.02	5.61	−1.44	0.0	0.00	0.0	0.00	67.4	8.00
Si I.....	6848.57	5.86	−1.75	22.9	7.58	43.1	8.01	0.0	0.00
S I	6748.78	7.87	−0.44	0.0	0.00	14.8	7.45	0.0	0.00
S I	6757.20	7.87	−0.29	0.0	0.00	19.8	7.54	0.0	0.00
Ca I	5867.57	2.93	−1.49	65.4	6.35	0.0	0.00	49.8	6.11
CaI	6439.08	2.52	0.39	211.4	5.97	188.5	5.91	183.7	5.79
Ca I	6449.82	2.52	−0.50	173.1	6.50	0.0	0.00	0.0	0.00
Ca I	6455.60	2.52	−1.29	118.9	6.51	0.0	0.00	0.0	0.00
Ca I	6499.65	2.52	−0.82	0.0	0.00	0.0	0.00	117.9	6.21
Ca I	6572.80	0.00	−4.32	0.0	0.00	124.4	6.69	0.0	0.00
Sc I	5671.83	1.45	0.56	0.0	0.00	68.2	3.21	0.0	0.00
Sc II	5526.82	1.77	0.19	115.9	2.98	0.0	0.00	101.2	3.12
Sc II	5640.99	1.50	−0.86	88.3	3.18	0.0	0.00	0.0	0.00
Sc II	5657.88	1.51	−0.29	0.0	0.00	112.5	3.30	96.7	3.19
Sc II	5684.20	1.51	−0.92	86.5	3.22	87.2	3.37	0.0	0.00
Sc II	6245.62	1.51	−1.05	0.0	0.00	85.0	3.38	71.0	3.30
Sc II	6279.74	1.50	−1.16	0.0	0.00	73.6	3.26	71.1	3.40
Sc II	6604.60	1.36	−1.14	0.0	0.00	80.9	3.18	81.1	3.37
Ti I	5490.16	1.46	−0.93	0.0	0.00	72.7	4.91	59.8	4.59
Ti I	5503.90	2.58	−0.19	59.8	5.15	0.0	0.00	0.0	0.00
Ti I	5662.16	2.32	−0.11	0.0	0.00	77.3	5.19	0.0	0.00
Ti I	5689.48	2.30	−0.47	51.8	4.97	58.3	5.16	46.2	4.86
Ti I	5978.55	1.87	−0.58	0.0	0.00	94.6	5.40	0.0	0.00
Ti I	6091.18	2.27	−0.42	0.0	0.00	66.3	5.18	48.6	4.78
Ti I	6126.22	1.07	−1.42	95.7	5.07	99.4	5.32	0.0	0.00
Ti I	6554.24	1.44	−1.22	0.0	0.00	91.1	5.36	69.8	4.91
V I.....	5627.64	1.08	−0.37	113.0	4.21	0.0	0.00	0.0	0.00
V I.....	5670.86	1.08	−0.42	109.0	4.17	0.0	0.00	0.0	0.00
V I.....	5703.59	1.05	−0.21	118.6	4.08	0.0	0.00	0.0	0.00
V I.....	6081.45	1.05	−0.58	105.8	4.16	82.4	3.90	62.0	3.44
V I.....	6090.22	1.08	−0.06	121.7	3.97	0.0	0.00	105.3	3.91
V I.....	6243.11	0.30	−0.98	0.0	0.00	0.0	0.00	104.0	3.75
V I.....	6251.83	0.29	−1.34	0.0	0.00	102.4	4.06	0.0	0.00
Cr I.....	5702.33	3.45	−0.68	0.0	0.00	0.0	0.00	47.3	5.65
Cr I.....	5781.19	3.32	−0.88	0.0	0.00	48.6	5.77	56.1	5.89
Cr I.....	5783.07	3.32	−0.40	79.9	5.75	0.0	0.00	0.0	0.00
Cr I.....	5784.98	3.32	−0.38	59.5	5.38	61.7	5.52	0.0	0.00
Cr I.....	5787.93	3.32	−0.08	0.0	0.00	0.0	0.00	74.0	5.48
Cr I.....	6330.10	0.94	−2.87	0.0	0.00	85.2	5.51	72.8	5.24
Cr I.....	6883.07	3.44	−0.42	84.6	5.91	0.0	0.00	66.4	5.71
Mn I.....	6013.50	3.07	−0.25	139.6	5.44	139.9	5.65	140.2	5.70
Mn I.....	6016.65	3.07	−0.09	156.4	5.54	0.0	0.00	0.0	0.00
Mn I.....	6021.80	3.08	0.03	173.5	5.65	0.0	0.00	0.0	0.00

TABLE 3—*Continued*

				333		978		979	
Element	λ	E. P.	log *gf*	EW (mÅ)	Abund.	EW (mÅ)	Abund.	EW (mÅ)	Abund.
Fe I	5491.84	4.19	−2.24	0.0	0.00	38.8	7.64	0.0	0.00
Fe I	5494.47	4.07	−1.96	0.0	0.00	54.4	7.53	0.0	0.00
Fe I	5522.45	4.21	−1.47	0.0	0.00	74.2	7.59	62.5	7.43
Fe I	5539.29	3.64	−2.59	0.0	0.00	0.0	0.00	66.9	7.99
Fe I	5547.00	4.22	−1.85	0.0	0.00	0.0	0.00	70.1	8.00
Fe I	5552.69	4.95	−1.69	0.0	0.00	0.0	0.00	12.4	7.24
Fe I	5560.22	4.43	−1.10	88.1	7.60	73.2	7.45	0.0	0.00
Fe I	5568.86	3.63	−2.82	41.8	7.57	34.4	7.48	0.0	0.00
Fe I	5577.03	5.03	−1.49	0.0	0.00	21.3	7.43	0.0	0.00
Fe I	5595.05	5.06	−1.69	0.0	0.00	12.3	7.36	0.0	0.00
Fe I	5608.98	4.21	−2.22	53.4	7.85	30.4	7.46	0.0	0.00
Fe I	5609.97	3.64	−3.09	0.0	0.00	21.0	7.46	0.0	0.00
Fe I	5611.36	3.63	−2.84	41.9	7.60	38.1	7.57	45.4	7.73
Fe I	5618.64	4.21	−1.34	94.7	7.72	78.2	7.54	0.0	0.00
Fe I	5619.61	4.39	−1.49	0.0	0.00	61.1	7.55	65.4	7.72
Fe I	5635.83	4.26	−1.59	0.0	0.00	69.6	7.67	0.0	0.00
Fe I	5636.70	3.64	−2.53	0.0	0.00	63.6	7.78	41.7	7.35
Fe I	5650.00	5.10	−0.80	0.0	0.00	0.0	0.00	54.0	7.56
Fe I	5651.48	4.47	−1.79	49.8	7.65	0.0	0.00	28.4	7.28
Fe I	5652.33	4.26	−1.77	0.0	0.00	67.7	7.82	61.0	7.75
Fe I	5677.69	4.10	−2.55	32.5	7.67	21.0	7.44	37.8	7.83
Fe I	5678.39	3.88	−2.88	0.0	0.00	19.5	7.48	0.0	0.00
Fe I	5680.24	4.19	−2.20	37.7	7.52	34.0	7.49	53.6	7.93
Fe I	5701.56	2.56	−2.16	0.0	0.00	0.0	0.00	125.9	7.56
Fe I	5717.84	4.28	−0.98	0.0	0.00	103.6	7.76	93.3	7.67
Fe I	5731.77	4.26	−1.10	102.8	7.67	0.0	0.00	80.6	7.50
Fe I	5738.24	4.22	−2.24	34.3	7.52	35.7	7.59	20.4	7.23
Fe I	5741.86	4.26	−1.69	84.0	7.91	66.7	7.70	73.2	7.93
Fe I	5742.96	4.18	−2.26	0.0	0.00	39.9	7.65	24.7	7.32
Fe I	5752.04	4.55	−0.92	0.0	0.00	85.5	7.64	81.9	7.67
Fe I	5759.26	4.65	−1.98	0.0	0.00	25.5	7.60	13.2	7.21
Fe I	5760.36	3.64	−2.46	0.0	0.00	0.0	0.00	61.5	7.71
Fe I	5778.46	2.59	−3.44	0.0	0.00	75.5	7.67	82.0	7.92
Fe I	5784.67	3.40	−2.53	66.3	7.42	0.0	0.00	0.0	0.00
Fe I	5793.92	4.22	−1.62	0.0	0.00	63.8	7.53	70.8	7.76
Fe I	5806.73	4.61	−0.93	71.3	7.32	83.8	7.68	0.0	0.00
Fe I	5811.91	4.14	−2.27	0.0	0.00	0.0	0.00	36.3	7.55
Fe I	5814.81	4.28	−1.81	67.4	7.75	43.2	7.38	37.4	7.27
Fe I	5835.11	4.26	−2.18	0.0	0.00	40.8	7.68	0.0	0.00
Fe I	5837.70	4.29	−2.21	26.6	7.42	35.6	7.64	0.0	0.00
Fe I	5849.69	3.69	−2.86	40.8	7.66	31.1	7.51	0.0	0.00
Fe I	5852.23	4.55	−1.36	0.0	0.00	0.0	0.00	51.7	7.45
Fe I	5855.09	4.61	−1.56	46.8	7.51	0.0	0.00	33.3	7.31
Fe I	5856.10	4.29	−1.57	67.7	7.53	0.0	0.00	73.1	7.85
Fe I	5858.78	4.22	−2.19	35.3	7.49	37.3	7.57	34.8	7.53
Fe I	5859.60	4.55	−0.63	117.4	7.78	0.0	0.00	0.0	0.00
Fe I	5861.11	4.28	−2.26	36.1	7.65	32.4	7.61	0.0	0.00
Fe I	5862.37	4.55	−0.42	0.0	0.00	0.0	0.00	107.3	7.63
Fe I	5879.49	4.61	−1.90	0.0	0.00	22.8	7.40	28.8	7.56
Fe I	5880.02	4.56	−1.85	0.0	0.00	0.0	0.00	27.5	7.42
Fe I	5881.28	4.61	−1.76	0.0	0.00	43.6	7.71	0.0	0.00
Fe I	5902.48	4.59	−1.86	48.7	7.82	34.8	7.60	49.4	7.94
Fe I	5905.68	4.65	−0.78	94.8	7.62	86.4	7.61	0.0	0.00
Fe I	5927.80	4.65	−1.07	71.9	7.50	71.1	7.60	65.1	7.56
FeI	5929.68	4.55	−1.16	87.1	7.75	67.4	7.50	69.7	7.63
Fe I	5930.19	4.65	−0.34	123.0	7.65	0.0	0.00	108.4	7.66
Fe I	5933.80	4.64	−2.05	23.1	7.56	17.9	7.44	26.6	7.68
Fe I	5934.66	3.93	−1.08	128.3	7.70	109.9	7.58	102.2	7.54
Fe I	5947.53	4.61	−1.95	22.5	7.41	0.0	0.00	0.0	0.00
Fe I	5969.57	4.28	−2.63	0.0	0.00	20.7	7.70	0.0	0.00
Fe I	5976.79	3.94	−1.30	0.0	0.00	0.0	0.00	103.9	7.81
Fe I	5984.83	4.73	−0.29	119.3	7.63	0.0	0.00	112.0	7.74
Fe I	6003.02	3.88	−1.02	129.1	7.60	124.0	7.71	127.4	7.85
Fe I	6007.97	4.65	−0.76	80.0	7.34	86.5	7.60	0.0	0.00

TABLE 3—*Continued*

				333		978		979	
ELEMENT	λ	E. P.	log *gf*	EW (mÅ)	Abund.	EW (mÅ)	Abund.	EW (mÅ)	Abund.
Fe I.....	6008.57	3.88	−0.92	120.4	7.35	0.0	0.00	116.7	7.59
Fe I.....	6015.24	2.22	−4.57	0.0	0.00	31.6	7.50	25.9	7.33
Fe I.....	6019.37	3.57	−3.14	43.7	7.84	21.8	7.43	0.0	0.00
Fe I.....	6027.06	4.07	−1.20	96.8	7.42	0.0	0.00	0.0	0.00
Fe I.....	6034.04	4.31	−2.30	20.9	7.38	27.3	7.57	0.0	0.00
Fe I.....	6054.08	4.37	−2.17	32.1	7.57	26.5	7.49	25.9	7.47
Fe I.....	6056.01	4.73	−0.46	116.0	7.75	0.0	0.00	109.0	7.86
Fe I.....	6065.49	2.61	−1.49	0.0	0.00	175.9	7.49	170.7	7.44
Fe I.....	6078.50	4.79	−0.38	127.2	7.90	100.8	7.64	0.0	0.00
Fe I.....	6079.02	4.65	−0.97	96.7	7.85	76.2	7.60	59.1	7.33
Fe I.....	6089.57	5.02	−0.87	73.4	7.75	0.0	0.00	60.5	7.67
Fe I.....	6093.65	4.61	−1.32	85.8	7.95	71.4	7.81	47.3	7.38
Fe I.....	6094.38	4.65	−1.56	0.0	0.00	0.0	0.00	42.8	7.56
Fe I.....	6096.67	3.98	−1.76	75.8	7.48	0.0	0.00	69.5	7.58
Fe I.....	6098.25	4.56	−1.81	0.0	0.00	49.6	7.82	0.0	0.00
Fe I.....	6120.26	0.91	−5.77	0.0	0.00	59.8	7.61	57.1	7.53
Fe I.....	6137.00	2.20	−2.91	133.5	7.54	0.0	0.00	0.0	0.00
Fe I.....	6151.62	2.18	−3.26	124.6	7.70	0.0	0.00	97.4	7.51
Fe I.....	6157.73	4.07	−1.26	0.0	0.00	0.0	0.00	95.3	7.72
Fe I.....	6246.33	3.60	−0.73	0.0	0.00	158.0	7.57	135.7	7.34
Fe I.....	6252.56	2.40	−1.64	0.0	0.00	183.5	7.45	0.0	0.00
Fe I.....	6270.23	2.86	−2.55	0.0	0.00	0.0	0.00	106.0	7.84
Fe I.....	6290.55	2.59	−4.27	37.6	7.70	42.6	7.83	46.0	7.88
Fe I.....	6297.80	2.22	−2.70	0.0	0.00	142.2	7.74	0.0	0.00
Fe I.....	6301.51	3.65	−0.72	0.0	0.00	146.9	7.44	140.9	7.42
Fe I.....	6311.50	2.83	−3.16	0.0	0.00	78.4	7.65	71.1	7.59
Fe I.....	6315.81	4.07	−1.67	0.0	0.00	75.6	7.58	67.5	7.51
Fe I.....	6322.69	2.59	−2.38	0.0	0.00	130.7	7.63	117.5	7.53
Fe I.....	6330.85	4.73	−1.22	0.0	0.00	0.0	0.00	62.5	7.72
Fe I.....	6335.34	2.20	−2.28	0.0	0.00	167.0	7.63	156.6	7.54
Fe I.....	6392.54	2.28	−3.97	0.0	0.00	68.4	7.61	0.0	0.00
Fe I.....	6411.66	3.65	−0.60	0.0	0.00	0.0	0.00	156.1	7.46
Fe I.....	6436.41	4.19	−2.31	42.0	7.67	38.5	7.65	0.0	0.00
Fe I.....	6518.37	2.83	−2.56	0.0	0.00	0.0	0.00	104.0	7.70
Fe I.....	6533.94	4.56	−1.28	0.0	0.00	0.0	0.00	62.5	7.57
Fe I.....	6591.31	4.59	−1.95	0.0	0.00	28.3	7.53	28.5	7.55
Fe I.....	6633.76	4.56	−0.81	0.0	0.00	97.6	7.70	0.0	0.00
Fe I.....	6667.43	2.45	−4.28	0.0	0.00	0.0	0.00	29.9	7.37
Fe I.....	6667.72	4.58	−2.01	0.0	0.00	36.9	7.76	43.7	7.93
Fe I.....	6699.14	4.59	−2.02	0.0	0.00	0.0	0.00	37.3	7.81
Fe I.....	6703.58	2.76	−3.00	0.0	0.00	0.0	0.00	100.2	7.94
Fe I.....	6704.48	4.22	−2.55	0.0	0.00	24.5	7.61	35.7	7.86
Fe I.....	6726.67	4.61	−1.05	0.0	0.00	69.6	7.44	64.3	7.43
Fe I.....	6733.15	4.64	−1.44	0.0	0.00	56.7	7.63	0.0	0.00
Fe I.....	6750.16	2.42	−2.58	0.0	0.00	131.8	7.56	125.9	7.60
Fe I.....	6753.47	4.56	−2.26	0.0	0.00	25.1	7.72	31.9	7.90
Fe I.....	6756.55	4.29	−2.69	0.0	0.00	22.4	7.78	0.0	0.00
Fe I.....	6786.86	4.19	−1.90	0.0	0.00	56.8	7.57	50.4	7.49
Fe I.....	6793.26	4.07	−2.34	0.0	0.00	0.0	0.00	35.7	7.47
Fe I.....	6796.12	4.14	−2.31	0.0	0.00	51.3	7.82	37.3	7.56
Fe I.....	6806.86	2.73	−3.14	0.0	0.00	0.0	0.00	84.5	7.70
Fe I.....	6810.27	4.61	−1.00	0.0	0.00	86.1	7.71	0.0	0.00
Fe I.....	6820.37	4.64	−1.16	0.0	0.00	0.0	0.00	84.5	7.99
Fe I.....	6843.66	4.55	−0.86	0.0	0.00	99.3	7.75	88.1	7.66
Fe I.....	6851.64	1.61	−5.22	57.1	7.74	0.0	0.00	49.4	7.65
Fe I.....	6855.72	4.61	−1.71	0.0	0.00	38.7	7.51	0.0	0.00
Fe I.....	6858.16	4.61	−0.95	0.0	0.00	80.6	7.55	78.3	7.62
Fe I.....	6861.95	2.42	−3.78	0.0	0.00	71.3	7.60	68.5	7.61
Fe I.....	6862.50	4.56	−1.43	0.0	0.00	60.8	7.60	55.5	7.56
Fe I.....	6880.63	4.15	−2.23	0.0	0.00	49.5	7.71	28.6	7.31
Fe I.....	6936.50	4.61	−2.14	0.0	0.00	29.2	7.75	15.7	7.38
Fe I.....	6960.32	4.59	−1.88	0.0	0.00	0.0	0.00	49.1	7.90
Fe I.....	6971.94	3.02	−3.35	0.0	0.00	64.6	7.76	0.0	0.00
Fe I.....	7010.35	4.58	−1.84	37.4	7.54	33.0	7.50	0.0	0.00

TABLE 3—*Continued*

				333		978		979	
ELEMENT	λ	E. P.	log gf	EW (mÅ)	Abund.	EW (mÅ)	Abund.	EW (mÅ)	Abund.
Fe I	7069.54	2.56	−4.20	0.0	0.00	39.8	7.63	34.3	7.49
Fe I	7114.56	2.69	−3.87	0.0	0.00	43.6	7.51	0.0	0.00
Fe I	7118.10	5.01	−1.50	0.0	0.00	38.1	7.73	28.4	7.56
Fe II.....	5991.38	3.15	−3.55	52.0	7.49	52.0	7.55	0.0	0.00
Fe II.....	6084.10	3.20	−3.80	0.0	0.00	31.9	7.36	34.2	7.65
Fe II.....	6113.33	3.21	−4.12	0.0	0.00	35.6	7.79	17.4	7.45
Fe II.....	6149.25	3.89	−2.72	0.0	0.00	0.0	0.00	37.1	7.43
Fe II.....	6247.56	3.87	−2.32	0.0	0.00	76.4	7.69	60.1	7.64
Fe II.....	6369.46	2.89	−4.21	0.0	0.00	34.4	7.50	0.0	0.00
Fe II.....	6383.72	5.55	−2.09	20.6	7.77	0.0	0.00	0.0	0.00
Fe II.....	6416.93	3.89	−2.70	0.0	0.00	0.0	0.00	53.2	7.86
Fe II.....	6432.68	2.89	−3.58	0.0	0.00	0.0	0.00	54.1	7.61
Fe II.....	6456.39	3.90	−2.10	0.0	0.00	84.7	7.68	0.0	0.00
Co I	5647.24	2.28	−1.56	0.0	0.00	68.8	5.00	74.0	5.25
Co I	6455.00	3.63	−0.25	57.5	4.91	60.5	5.04	36.2	4.60
Ni I	5578.73	1.68	−2.57	0.0	0.00	118.4	6.53	0.0	0.00
Ni I	5587.87	1.93	−2.39	0.0	0.00	98.3	6.17	0.0	0.00
Ni I	5589.37	3.90	−1.15	49.9	6.13	0.0	0.00	0.0	0.00
Ni I	5593.75	3.90	−0.78	0.0	0.00	64.3	6.13	0.0	0.00
Ni I	5643.09	4.16	−1.25	0.0	0.00	39.3	6.37	0.0	0.00
Ni I	5748.36	1.68	−3.25	0.0	0.00	94.5	6.61	67.7	6.15
Ni I	5760.84	4.10	−0.81	0.0	0.00	54.7	6.18	0.0	0.00
Ni I	5805.23	4.17	−0.60	0.0	0.00	65.4	6.26	0.0	0.00
Ni I	5847.01	1.68	−3.44	0.0	0.00	74.3	6.37	0.0	0.00
Ni I	5996.74	4.23	−1.06	0.0	0.00	46.1	6.39	38.3	6.29
Ni I	6053.69	4.23	−1.07	0.0	0.00	0.0	0.00	43.8	6.43
Ni I	6086.29	4.26	−0.47	72.3	6.25	0.0	0.00	0.0	0.00
Ni I	6108.13	1.68	−2.47	130.0	6.25	124.6	6.40	122.2	6.56
Ni I	6111.08	4.09	−0.83	72.9	6.42	60.6	6.28	57.4	6.33
Ni I	6128.98	1.68	−3.39	74.9	6.15	82.4	6.43	0.0	0.00
Ni I	6130.14	4.26	−0.98	0.0	0.00	49.6	6.40	0.0	0.00
Ni I	6322.17	4.15	−1.21	0.0	0.00	0.0	0.00	38.6	6.34
Ni I	6327.60	1.68	−3.08	0.0	0.00	0.0	0.00	95.4	6.53
Ni I	6482.81	1.93	−2.78	0.0	0.00	0.0	0.00	87.2	6.35
Ni I	6586.32	1.95	−2.78	0.0	0.00	103.5	6.53	100.0	6.65
Ni I	6598.61	4.23	−0.93	0.0	0.00	53.3	6.37	0.0	0.00
Ni I	6767.78	1.83	−2.06	0.0	0.00	148.0	6.45	138.9	6.45
Ni I	6772.32	3.66	−0.96	0.0	0.00	0.0	0.00	90.0	6.63
Y II.....	5544.62	1.74	−1.09	0.0	0.00	23.2	2.33	30.5	2.64
Ba II.....	6496.91	0.60	−0.38	0.0	0.00	0.0	0.00	120.6	2.17

NOTE.—Abundances are derived from the equivalent line width [log $n(A)$, on the scale for which log $n(H) = 12$].

used to derive the best set of atmospheric parameters listed in Table 2. Effective temperatures were derived directly from the spectra, imposing Fe I lines of different excitation (several tens for each star) to provide the same temperatures. Figure 3*a* shows the run of abundances from Fe I lines with excitation potential for star 978: there is no discernible trend. Internal error estimates in temperatures are obtained directly from the errors in the linear regression fits and are ± 68 K, corresponding to 1 σ rms uncertainty of 0.015 dex eV^{-1} in the slope. Systematic errors might be larger and mainly ascribed to the set of adopted model atmospheres (Kurucz 1995).

In addition, a number of Fe II lines were measured in each star, allowing an estimate of surface gravities log g from the equilibrium of ionization of Fe, which is very well derived from our Fe lines. Internal errors include the contribution from both the above uncertainties in the adopted temperature and the errors in EWs of individual lines: the quadratic sums provide an internal error of ± 0.19 dex in log g. Our use of the LTE approximation in the analysis is not of concern for these stars (see Gratton et al. 1999); however, systematic errors can be present, again mainly related to the adopted model atmospheres.

The following exercise shows that the assumed temperature scale leads to a reasonable internal consistency of data. The (average) absolute magnitude of the program stars is $M_V = +0.6$, according to their apparent magnitude and to the distance modulus of $(m - M)_V = 12.35$ by Rosvick & VandenBerg (1998) and in agreement with the average value for clump stars measured by *Hipparcos*. The bolometric correction appropriate for the temperature, gravity, and metal abundances of the program stars, derived from Kurucz (1995) is BC $= -0.44$ mag. This leads to an assumed luminosity of the program stars of log $L/L_\odot =$ 1.82, and, assuming a mass of 1.5–1.6 $M_\odot$ (appropriate for a clump star in a 2.5 Gyr old cluster; see Rosvick & Vanden-

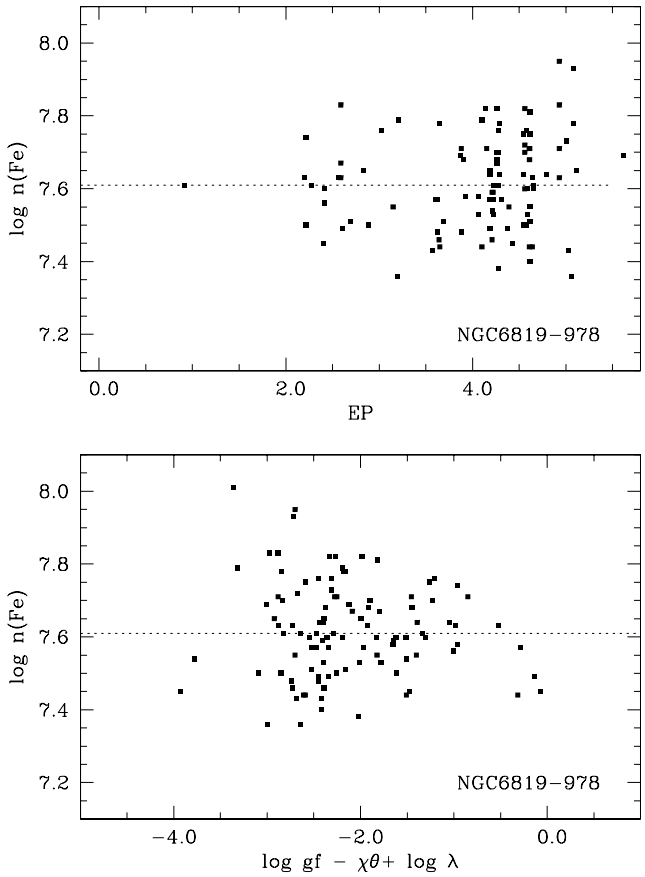

FIG. 3.—Trends of abundances from individual Fe I lines with excitation potential (*top*) and expected line strength (*bottom*) for star 978.

Berg 1998), we obtain an expected gravity for the program stars of $\log g = 2.5$, in reasonable agreement with the observed value. Note that if we instead decrease $T_{\rm eff}$ by 100 K, we obtain a good ionization equilibrium for a gravity of $\log g \sim 2.3$, which implies an absolute magnitude of $M_V \sim +0.3$, too bright in our opinion for clump stars in an old open cluster. This exercise thus suggests that the adopted temperature scale might be overestimated but only slightly (by $\simeq 50$ K); such a small error would cause our [Fe/H] value to be overestimated by only 0.03 dex. Hereafter, we will assume that systematic errors are not larger than the internal errors of ± 70 K.

Microturbulent velocities v_t were obtained by compensating any trend in the derived abundances from Fe I lines with the expected line strength (see Magain 1984). Results for star 978 are shown in Figure 3*b*. Because of the large number of measured Fe I lines and the high quality of measurements, internal error bars in the derived values of v_t are almost negligible (± 0.07 km s^{-1}, average from the three stars).

3.3. *Abundances*

Table 4 lists the abundances obtained for the individual stars, as well as the average values for the cluster. Sensitivities of these abundances to changes in the atmospheric parameters are listed in Table 5 and were used to estimate the internal errors in our abundances. These errors are listed in the last column of Table 4 and were obtained by summing quadratically the contribution due to each atmospheric parameter (assuming uncertainties of 70 K in $T_{\rm eff}$, 0.19 dex in log g, 0.05 dex in [A/H], and 0.07 km s^{-1} in v_t; see the last column of Table 5) and that due to the line-to-line scatter (we assumed 0.15 dex); the value was then

TABLE 4

AVERAGE ABUNDANCES

		333				978				979				
El.	Sun	*N*	Abund.	rms	Overab.	*N*	Abund.	rms	Overab.	*N*	Abund.	rms	Overab.	⟨[A/Fe]⟩
Fe I.....	7.52	49	7.62	0.16	+0.10	90	7.60	0.12	+0.08	90	7.61	0.20	+0.09	+0.09 ± 0.03
Fe II	7.52	2	7.63	0.14	...	6	7.60	0.15	...	6	7.61	0.16	...	...
Na I	6.23	2	6.68	0.11	+0.35	1	6.96	...	+0.65	3	6.72	0.37	+0.40	+0.47 ± 0.07
Mg I.....	7.48	1	7.50	...	−0.08	1	7.65	...	+0.09	3	7.20	0.10	−0.37	−0.12 ± 0.07
Al I	6.30	1	6.35	...	−0.05	1	6.44	...	+0.06	2	6.17	0.32	−0.22	−0.07 ± 0.07
Si I.....	7.55	7	7.65	0.10	+0.03	8	7.82	0.14	+0.19	8	7.96	0.16	+0.32	+ 0.18 ± 0.04
Ca I	6.18	4	6.34	0.25	+0.06	2	6.30	0.55	+0.04	3	6.04	0.22	−0.23	−0.04 ± 0.06
Sc I	3.10	...	...	...	...	1	3.21	...	+0.03	...	...	...	...	+0.02 ± 0.13
Sc II	3.10	3	3.13	0.13	−0.07	5	3.30	0.08	+0.12	5	3.28	0.12	+0.06	+ 0.04 ± 0.04
Ti I	4.94	3	5.06	0.09	+0.02	7	5.22	0.16	+0.20	4	4.78	0.14	−0.25	−0.01 ± 0.04
V I.....	3.93	5	4.12	0.10	+0.09	2	3.98	0.12	−0.03	3	3.70	0.24	−0.32	−0.09 ± 0.07
Cr I.....	5.63	3	5.68	0.27	−0.05	3	5.60	0.14	−0.11	5	5.59	0.25	−0.13	−0.10 ± 0.05
Mn I.....	5.47	3	5.54	0.11	−0.03	1	5.66	...	+0.11	1	5.70	...	+0.14	+ 0.07 ± 0.08
Co I	4.94	1	4.91	...	−0.13	2	5.02	0.03	0.00	2	4.93	0.45	−0.10	−0.08 ± 0.05
Ni I.....	6.25	5	6.24	0.11	−0.11	16	6.37	0.14	+0.04	11	6.43	0.15	+0.09	+ 0.01 ± 0.02
Y II	2.24	...	...	...	...	1	2.34	...	+0.02	1	2.64	...	+0.31	+ 0.16 ± 0.10
Ba II.....	2.34	...	...	...	...	...	...	...	...	1	2.16	...	− −0.27	−0.27 ± 0.15

NOTES.—The adopted solar abundances in the second column were obtained from an inverted solar analysis using Kurucz model atmospheres and equivalent widths from the literature for the same set of lines as that used for the stars. For each star we list *N*, the number of lines, the average abundance [on the scale log $n(A)$, where log $n(H) = 12$], the rms of individual lines around this average value, and the overabundance with respect to Fe, except that we list the [Fe/H] value for Fe. The last column lists the average overabundances ([Fe/H] values for Fe) for NGC 6819; the error bars were obtained as explained in the text.

TABLE 5

SENSITIVITY OF ABUNDANCES TO ATMOSPHERIC PARAMETERS

Element	$\Delta T_{\rm eff}$ (+100 K)	$\Delta \log g$ (+0.3 dex)	Δ[A/H] (+0.1 dex)	Δv_t (+0.2 km^{-1})	Total
[Fe/H]I	+0.059	+0.016	+0.010	−0.057	0.048
[Fe/H]II	−0.082	+0.159	+0.037	−0.061	0.128
[Na/Fe]	+0.029	−0.066	−0.010	−0.018	0.129
[Mg/Fe]	−0.015	−0.016	−0.003	+0.029	0.121
[Al/Fe]	+0.013	−0.032	−0.013	+0.016	0.122
[Si/Fe]	−0.078	+0.036	+0.010	+0.016	0.072
[Ca/Fe]	+0.082	−0.072	−0.016	−0.046	0.113
[Sc/Fe]	+0.070	−0.037	−0.009	−0.043	0.077
[Ti/Fe]	+0.076	−0.024	−0.018	−0.028	0.071
[V/Fe]	+0.107	−0.016	−0.022	−0.049	0.114
[Cr/Fe]	+0.050	−0.022	−0.016	−0.004	0.079
[Mn/Fe]	+0.035	−0.072	−0.003	−0.080	0.133
[Co/Fe]	+0.001	+0.031	+0.003	−0.008	0.087
[Ni/Fe]	−0.013	+0.034	+0.006	−0.040	0.040
[Y/Fe]	+0.067	−0.027	+0.001	+0.043	0.130

divided by the square root of the number of stars used to estimate abundances.

The average Fe abundance for NGC 6819 is [Fe/H] = +0.09 ± 0.03, the three stars yielding very similar results. Element-to-element abundance ratios are generally close to solar (within twice the internal error; note that abundances for V, Mn, and Co include corrections for the quite large hyperfine structure of their lines). There are two exceptions:

1. We get a slight overabundance of Si (on average, [Si/Fe] = +0.18 ± 0.04). This result is obtained from a rather large number of lines and seems reasonably sound.

2. We find quite a large Na excess (on average, [Na/Fe] = +0.47 ± 0.07). This value includes a small non-LTE correction (<0.05 dex), computed according to Gratton et al. (1999). A partial confirmation of the results of the equivalent width–based abundance analysis comes from comparisons of the observed spectra with synthetic spectra. An example of such a comparison is shown in Figure 4, where the spectral region 6150–6166 Å is presented and compared with results of spectral synthesis computations. Note the good match of the Fe I lines. Na and Si lines are clearly stronger than predicted for a solar-scaled composition, indicating an overabundance with respect to Fe. However, the excess we would derive from this figure is about [Na/Fe] ~ +0.3, a bit lower than that given by the equivalent widths. Similar excesses of Na have been found for Population I supergiants (see e.g., Sasselov 1986); however, the clump stars in NGC 6819 are much less massive than those considered by Sasselov.

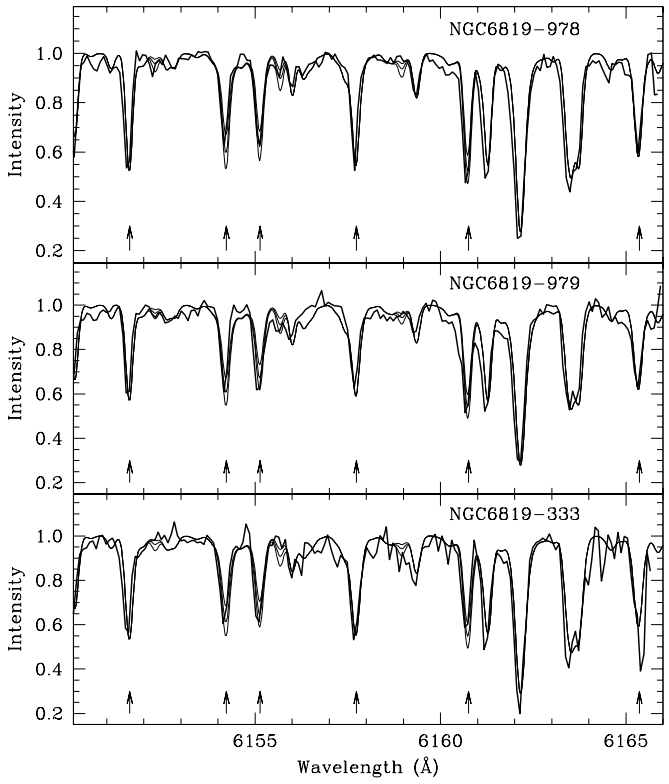

FIG. 4.—Spectra of the observed stars in the region 6150–6165 Å (*thick lines*) compared with synthetic spectra computed with the appropriate atmospheric parameters and abundances, and three different values of Na and Si abundances ([Na/Fe] = 0.0, 0.3, and 0.6; [Si/Fe] = 0.0, 0.3, and 0.6; *thin lines*). Lines of Na, Si and Fe are marked by arrows (Na I λλ6154.230, 6160.753, Si I λ6155.135, Fe I λλ6151.623, 6157.733, 6165.363). Note the good match of the Fe I lines. Na and Si are clearly overabundant with respect to Fe.

4. SUMMARY AND CONCLUSIONS

We can use our temperatures derived from line excitation (and hence a reddening-free parameter) to derive the interstellar reddening toward NGC 6819. This can be done by comparing the observed $B-V$ colors with those predicted by models (Kurucz 1995). There might be some systematic errors in such reddening derivations, since they would depend on the accuracy of the colors computed by model atmospheres and on possible errors in the *gf* values. However, this zero-point offset (itself a function of temperature) may be determined by observation of a comparison sample of nearby unreddened clump stars, analyzed by strictly following the same procedure described here. We did this for a sample of 12 bright clump stars with accurate parallaxes from *Hipparcos* (Carretta et al. 2001). This comparison sample overlaps in temperature and metal abun-

dance the stars of NGC 6819, so that no extrapolation was required. Using this procedure, we derive an average reddening for our three clump stars of $E(B-V) = 0.142 \pm 0.044$ (three stars, rms = 0.076 mag). This value agrees very well with that obtained recently by Rosvick & VandenBerg [$E(B-V) = 0.16$] in their accurate study based on good-quality CCD photometry. Previous determinations were contradictory, ranging, e.g., from $E(B-V) = 0.12$ (Burkhead 1971) to $E(B-V) = 0.28$ (Auner 1974), and were based on more uncertain photographic photometry.

Our determination of the metallicity for NGC 6819 ([Fe/H] $= +0.09 \pm 0.03$) is only slightly higher than the value obtained by Rosvick & VandenBerg (1998) from an analysis of the color-magnitude diagram ([Fe/H] $= -0.05$) and seems to agree very well with the value given by Twarog, Ashman, & Anthony-Twarog (1997; [Fe/H] $= +0.07 \pm 0.05$) and based on a revision of the low-dispersion spectroscopic data by Friel & Janes (1993). In fact the latter agreement is based on a value for the reddening [$E(B-V) = 0.28 - 0.30$] much higher than ours, derived from quite old data and explicitly admitted to be highly uncertain. Had they adopted a lower value for the reddening, their metallicity would have also been lower ([Fe/H] $\simeq -0.05$ or -0.10; see Rosvisk & VandenBerg 1998), but the discrepancy is fairly modest.

Our values for the metallicity and reddening of NGC 6819 are close enough to the values presented by Rosvick & VandenBerg that no new analysis of distance modulus and age for this cluster seems required. We must recall, however, that the age and distances derived from isochrone fitting to the cluster color-magnitude diagram are highly sensitive to the adopted stellar models. Finally, we point out that our reddening and metallicity agree perfectly with those recently adopted by Sarajedini (1999) in his discussion of the dependence of the luminosity of the clump on age and metallicity.

NGC 6819 hence appears to be a cluster with galactocentric distance (8–9 kpc) similar to that of the Sun, metallicity moderately higher, and age slightly younger. These features make it consistent with standard age-metallicity relations and abundance gradients.

We acknowledge the use of the BDA, the open cluster database maintained by J. C. Mermilliod. This research has made use of the SIMBAD database, operated at CDS, Strasbourg, France. We thank the referee for thorough comments and useful suggestions. Financial support has been provided by the Italian MURST, through COFIN-1998 under the stellar evolution project. Partial support by Consorzio Nazionale per l'Astronomia e l'Astrofisica is also acknowledged.

REFERENCES

Auner, G. 1974, A&AS, 13, 143
Bragaglia, A., Tosi, M., Marconi, G., & Carretta, E. 2001, in The Evolution of the Milky Way: Stars vs. Clusters, ed. F. Giovannelii & F. Matteucci (Dordrecht: Kluwer), in press
Burkhead, M. S. 1971, AJ, 76, 251
Carretta, E., Cohen, J. G., Gratton, R. G., & Behr, B. B. 2001, in preparation
Friel, E. D. 1995, ARA&A, 33, 381
Friel, E. D., & Janes, K. A. 1993, A&A, 267, 75
Gratton, R. G. 1988, Rome Obs. Preprint Ser. 29
Gratton, R. G., Carretta, E., Gustafsson, B., & Eriksson, K. 1999, A&A, 350, 955
Gratton, R. G., et al. 2001, in preparation
Kurucz, R. L. 1995, CD-ROM 13, Opacities for Stellar Atmosphees: Abundance Sample (Cambridge: Smithsonian Astrophys. Obs.)
Luhman, K. L., Rieke, G. H., Young, E. T., Cotera, A. S., Chen, H., Rieke, M. J., Schneider, G., & Thompson, R. I. 2000, ApJ, 540, 1016
Magain, P. 1984, A&A, 134, 189
Mayor, M. 1976, A&A, 48, 301
Mermilliod, J.-C. 1995, in Information and On-Line Data in Astronomy, ed. D. Egret & M. A. Albrecht (Dordrecht: Kluwer), 127
Panagia, N., & Tosi, M. 1981, A&A, 96, 306
Rosvick, J. M., & VandenBerg, D. A. 1998, AJ, 115, 1516
Sanders, W. L. 1972, A&A, 19, 155
Sandrelli, S., Bragaglia, A., Tosi, M., & Marconi, G. 1999, MNRAS, 309, 739
Sarajedini, A. 1999, AJ, 118, 2321
Sasselov, D. D. 1986, PASP, 98, 561
Twarog, B. A., Ashman, K., & Anthony-Twarog, B. 1997, AJ, 114, 2556